Bioorganic & Medicinal Chemistry 19 (2011) 1721–1728

Contents lists available at ScienceDirect

Bioorganic & Medicinal Chemistry

journal homepage: www.elsevier.com/locate/bmc

Synthesis and evaluation of cyclic RGD-boron cluster conjugates to develop tumor-selective boron carriers for boron neutron capture therapy

Sadaaki Kimura [a,†], Shin-ichiro Masunaga [b], Tomohiro Harada [a], Yasuo Kawamura [a], Satoshi Ueda [a], Kensuke Okuda [a], Hideko Nagasawa [a,*]

[a] Laboratory of Medicinal & Pharmaceutical Chemistry, Gifu Pharmaceutical University, 1-25-4 Daigaku-nishi, Gifu 501-1196, Japan
[b] Radiation Oncology Research Laboratory, Research Reactor Institute, Kyoto University, Asashiro-nishi 2-1010, Kumadori-cho, Sennan-gun, Osaka 590-0494, Japan

ARTICLE INFO

Article history:
Received 23 December 2010
Revised 11 January 2011
Accepted 12 January 2011
Available online 18 January 2011

Keywords:
Integrin αvβ3
Boron neutron capture therapy (BNCT)
o-Carborane
Cyclic RGD

ABSTRACT

Boron-containing agents play a key role in successful boron neutron capture therapy (BNCT). Icosahedral boron cluster-Arg-Gly-Asp (RGD) peptide conjugates were designed, synthesized, and evaluated for the biodistribution to develop tumor-selective boron carriers. Integrin αvβ3 is an attractive target for anti-tumor drug delivery because of its specific expression in proliferating endothelial and tumor cells of various origins. We, therefore, selected a c(RGDfK) moiety recognizing αvβ3 as an active tumor-targeting device to conjugate with icosahedral boron-10 clusters, disodium mercaptododecaborate (BSH) or *o*-carborane as a thermal neutron-sensitizing unit. Preparation of *o*-carborane derivatives involved microwave irradiation, and resulted in high yields in a short time. An in vitro cell adhesion assay on αvβ3-positive U87MG and SCCVII cells demonstrated the high binding affinity of conjugates to integrin αvβ3 (IC_{50} = 0.19–2.66 μM). Biodistribution experiments using SCCVII-bearing mice indicated that GPU-201 showed comparable tumor uptake and a significantly longer retention in tumors compared with BSH. These results suggest that GPU-201 is a promising candidate for use in BNCT.

1. Introduction

Boron neutron capture therapy (BNCT) is, in principle, the most promising modality for cancer treatment provided that a sufficient amount of boron-10 (^{10}B) can be accumulated in the target tumor and a sufficient number of very-low-energy thermal neutrons can be delivered there. BNCT is based on the neutron capture and fission reaction of non-radioactive ^{10}B, [^{10}B (^{1}n, α)^{7} Li]. This results in selective boron-localized cell killing because the particles generated in this reaction have a short range of approximately 14 μm (the approximate diameter of 1–2 cells), and carry high linear energy transfer.[1,2] Therefore, tumor-selective delivery of a sufficient amount of ^{10}B atoms is essential for the success of BNCT.

Disodium mercaptododecaborate (BSH)[3,4] and *p*-boronophenylalanine (BPA)[5,6] are available ^{10}B carriers for clinical investigation, and currently undergoing clinical trials[7] for BNCT. Both boron carriers are, however, not ideal for delivering a therapeutic amount of ^{10}B throughout the target tumor because they tend to be washed out immediately after injection.[8,9] We recently developed tumor-targeting ^{10}B carriers such as 2-nitroimidazole-sodium borocaptate-^{10}B conjugate[10] and hypoxia-specific cytotoxic bioreductive agent sodium–^{10}B-dodecaborate conjugates.[11] In the development of these compounds, we focused on the tumor microenvironment characterized by regions of hypoxia, low nutrition, and acidosis due to incomplete blood-vessel networks as a general target of solid tumors regardless of cancer types.[12] Meanwhile several boron carriers such as molecular-targeted agents toward somatostatin,[13,14] folate,[15,16] transferrin,[17] VEGF,[16,18] or EGF[16,19,20] receptors as well as nucleoside,[21] aminoacid,[22] or porphyrin derivatives[23,24] have been developed as tumor-targeting BNCT agents.[25]

In recent years, great progress has been made towards targeting integrins in cancer treatment.[26] Integrins are a superfamily of heterodimeric transmembrane receptors comprising 19 α-subunits and 9 β-subunits which participate in cell–cell and cell–matrix interactions.[27] Integrin regulates a diverse array of cellular functions related to the progression, angiogenesis, and metastasis in the tumor microenvironment.[28,29] Among the integrin family, integrin $\alpha_v\beta_3$ is the most attractive target for anti-tumor drug delivery,[30] and tumor imaging[31] with PET[32–34] SPECT,[35–37] optical imaging,[38,39] and MRI[40] due to its specific expression on proliferating endothelial cells and tumor cells of various origins.[27,29] Therefore, we developed new tumor-selective boron carriers bearing integrin-binding Arg-Gly-Asp (RGD) consensus motifs for enhancing the tumor-specific uptake of ^{10}B atoms. We carried out the design, synthesis, and pharmacokinetic evaluation of novel boron carriers conjugated with cyclic RGD peptides directed to integrin $\alpha_v\beta_3$.

* Corresponding author. Tel./fax: +81 58 230 8112.
E-mail address: hnagasawa@gifu-pu.ac.jp (H. Nagasawa).
† Present address: Functional Imaging Division, National Cancer Center Hospital East, Kashiwanoha 6-5-1, Kashiwa, Chiba 277-8577, Japan.

0968-0896/$ - see front matter © 2011 Elsevier Ltd. All rights reserved.
doi:10.1016/j.bmc.2011.01.020

2. Results and discussion

2.1. Molecular design

RGD is the consensus sequence of matrix proteins for binding integrins at the cell surface. Kessler and coworkers developed c(RGDfV) as the first highly active and selective $\alpha_v\beta_3$ antagonist,[41] which acts as a lead structure for stereoisomeric peptidomimetics. c(RGDfK), and c(RGDfC) were developed to be functionalized with various linker molecules through the amino or mercapto group on the lysine or cysteine residue.[32] Therefore, we selected the c(RGDfK) moiety as an active tumor-targeting device and two icosahedral boron-10 clusters, that is, disodium mercaptododecaborate (BSH) or 1,2-dicarba-*closo*-dodecaborane (*o*-carborane), in terms of the difference in physicochemical properties as a thermal neutron-sensitizing unit. These tumor-targeting units and sensitizing units were conjugated through suitable linkers, which can control distance, orientation, flexibility, and physicochemical properties (Fig. 1). More recently, multimeric RGD compounds such as E[c(RGDfK)]$_2$ or {E[c(RGDfK)]$_2$}$_2$ have been exploited to improve the targeting potential.[42–44] Hence, we also used RGD-dimers such as E[c(RGDfK)]$_2$ to increase tumor accumulation. BSH is an extremely hydrophilic dianion comprising 12 boron atoms with a mercapto group, whereas *o*-carborane (icosahedra comprising 10 boron atoms and two adjacent carbon atoms) is hydrophobic comparable with benzene. Various combinations of boron clusters having different physicochemical properties and cyclic RGDs through suitable linkers are expected to improve the pharmacokinetics and tumor uptake of boron carriers.

2.2. Chemistry

To compare the effects of RGD-monomer and -dimer on integrin selectivity and tumor uptake, c(RGDfK) and E[c(RGDfK)]$_2$ were prepared. Additionally, the randomized sequence peptide c(KGfDR) was prepared as a control. To prepare cyclic RGD peptide, the linear-protected peptide, H-Asp(*t*-Bu)-D-Phe-Lys(Boc)-Arg(Pbf)-Gly-OH, was obtained by assembling Fmoc-Gly-(2-Cl)Trt resin by the conventional Fmoc strategy, and cleaving with 20% 1,1,1,3,3,3-hexafluoroisopropanol in DCM. Cyclization of the linear-protected peptide was carried out using diphenylphosphoryl azide in the presence of $NaHCO_3$ under high dilution conditions followed by treatment with 95% TFA to afford the desired c(RGDfK) in quantitative yield. Preparation of E[c(RGDfK)]$_2$ was achieved by the reaction of Boc-Glu(OSu)-OSu with the amino group of lysine residue on c(RGDfK) and subsequent removal of the Boc group.

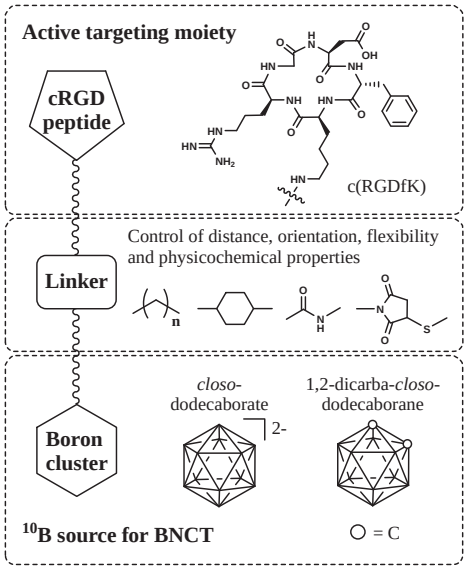

Figure 1. Molecular design of boron carrier.

RGD peptide-BSH conjugates were prepared in a two-step process: conjugation of peptide with linker-bearing maleimide moiety and Michael addition of the SH group on BSH to the maleimide moiety (Scheme 1). c(RGDfK) or E[c(RGDfK)]$_2$ were conjugated with maleimide linker **1** derived from β-alanine to afford **2** and **4**, respectively. Subsequent reactions of maleimide on these cyclic peptide-linker conjugates with BSH were carried out in phosphate buffer (pH 7) to give **3**: GPU-51 and **5**: GPU-180. The Michael addition was successfully performed in aqueous media with low dimerization of BSH to BSSB, which was a measurable side reaction in organic media such as DMF or MeCN using an organic base. Similarly, a cyclic RGD-BSH conjugate-bearing tranexamic acid-based linker was synthesized. Maleimido-tranexamic acid linker **6**[45] was converted to the corresponding activated ester **7**, which was conjugated with c(RGDfK) to give **8**. Conjugate addition of BSH was undertaken in the same manner to give **9**: GPU-176. Attempts to synthesize E[c(RGDfK)]$_2$-BSH conjugate via a tranexamic acid linker were not successful because of the instability of the isolated product.

The syntheses of c(RGDfK)-linked *o*-carborane from 5-hexyn-1-ol (**10**) are summarized in Scheme 2. Protection of alcohol **10** with a benzyl group was employed to afford the corresponding benzyl ether **11**. Subsequent formation of a carborane cage under microwave irradiation gave carboranyl ether **12** in high yield within a very short period (30 min) compared with the conventional synthetic method (40%, 2.5 days). Hydrogenolysis of **12** and oxidization of **13** with CrO_3/H_5IO_6[46] afforded the corresponding carboxylic acid **14**. After transformation of **14** to activated ester **15**, conjugation of c(RGDfK) or E[c(RGDfK)]$_2$ with **15** produced **16**: GPU-49 and **17**: GPU-189, respectively. *o*-Carborane has two adjacent carbon atoms thereby enabling construction of a different type of RGD dimer by the attachment of c(RGDfK) to each carbon atom via a linker. Lithiation of **12** followed by alkylation with **18** gave symmetrically 1,2-bifunctionalized *o*-carboarne **19**, which was deprotected by hydrogenolysis using cyclohexene under reflux conditions. Oxidation of diol **20** afforded the corresponding di-carboxylic acid **21**. Conversion to di-activated ester **22** using HOBt and EDCI was performed; subsequent reaction with c(RGDfK) gave the symmetric RGD-dimer **23**: GPU-201. Similarly, the randomized peptide sequence c(KGfDR) was coupled with di-activated ester **22** to give **24** GPU-205 as the corresponding negative control of GPU-201.

2.3. Biology

2.3.1. Cell adhesion assay

Binding affinities and specificities of all RGD-boron conjugates to integrin $\alpha_v\beta_3$ were evaluated using a cell adhesion assay[33] on $\alpha_v\beta_3$-positive U87MG human glioblastoma cells (see the western blotting data in Fig. S1 in Supplementary data). Vitronectin is a specific ligand for integrin $\alpha_v\beta_3$.[27] All conjugates except the non-RGD conjugate GPU-205 inhibited the adhesion of U87MG cells on vitronectin-coated plates in a concentration-dependent manner (Fig. 2). As shown in Figure 3C, IC_{50} values of BSH conjugates GPU-51, -176, and -180 were 1.08 ± 0.34 μM, 0.31 ± 0.03 μM, and 0.44 ± 0.04 μM, and those of *o*-carborane conjugates GPU-49, -189, and -201 were 2.66 ± 0.85 μM, 0.39 ± 0.03 μM, and 0.61 ± 0.08 μM, respectively, which were comparable to the values reported for other multimeric RGD conjugates previously.[33] Binding affinities of RGD-monomers GPU-49 and -51 except for GPU-176 were lower than those of the RGD-dimers GPU-180, -189 and -201. Multimeric RGD peptides can significantly enhance

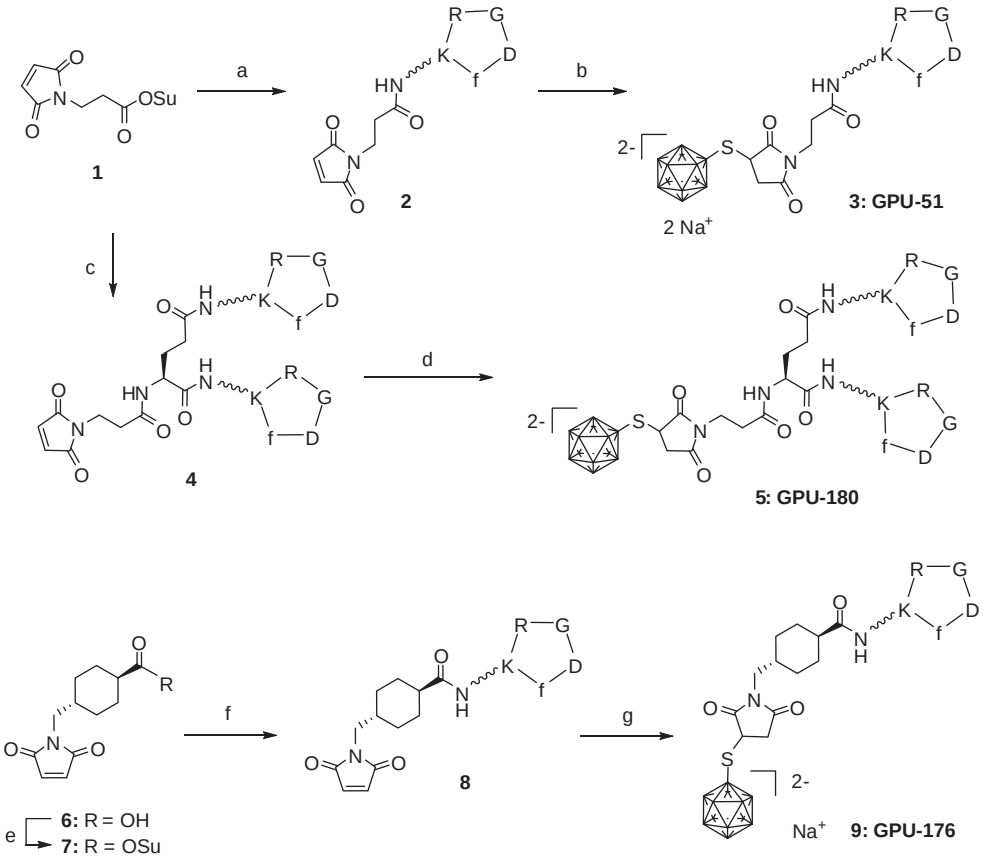

Scheme 1. Reagents and conditions: (a) c(RGDfK), DIPEA, DMF, rt, 84%; (b) B-10 enriched BSH, pH 7 phosphate buffer, rt, 56%; (c) E[c(RGDfK)$_2$], DIPEA, DMF, rt, 86%; (d) B-10 enriched BSH, pH 7 phospate buffer, rt, 71%; (e) HOSu, EDCI·HCl, DCM, rt; (f) c(RGDfK), DIPEA, DMF, rt, 40% (from **6**); (g) B-10 enriched BSH, pH 7 phosphate buffer, rt, 45%.

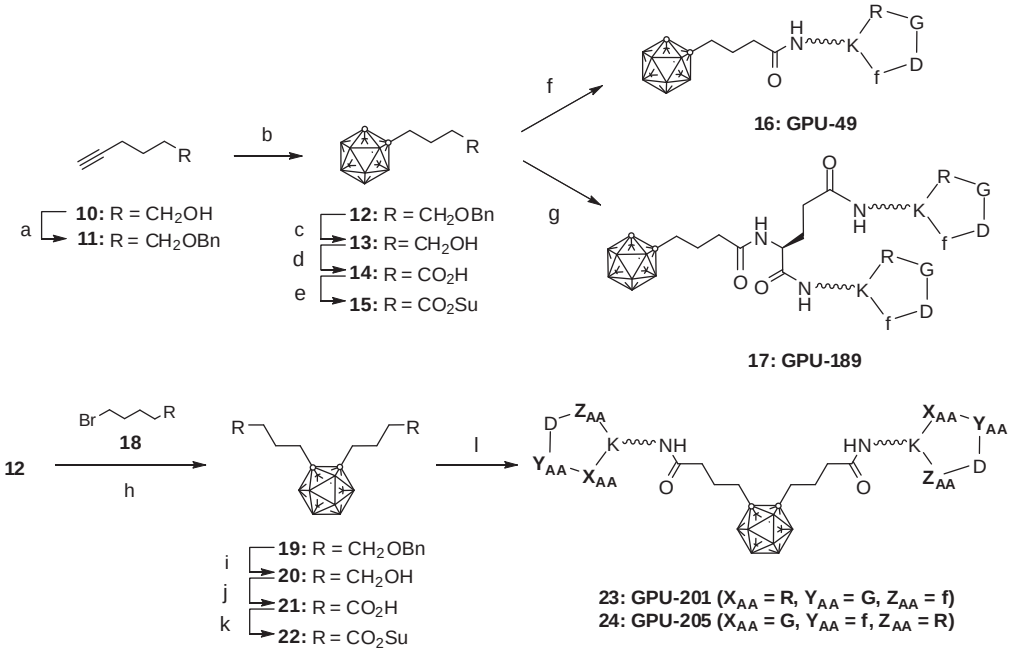

Scheme 2. Reagents and conditions: (a) (i) NaH, THF, 0 °C to rt; (ii) BnBr, THF, rt, 52%; (b) $B_{10}H_{14}$, *N*,*N*-dimethylaniline, chlorobenzene, 80 °C, microwave, 88%; (c) H_2, 10% Pd/C, MeOH, AcOH, rt, 86%; (d) H_5IO_6, CrO_3, wet MeCN, rt, quant.; (e) HOSu, EDCI·HCl, DCM, rt, 97%; (f) c(RGDfK), DIPEA, DMF, rt, 86%; (g) E[c(RGDfK)$_2$], DIPEA, DMF, rt, 68%; (h) (i) *n*-BuLi, THF, −40 °C to rt; (ii) **18**, LiI, rt, 65%; (i) cyclohexene, Pd/C, EtOH, reflux, 88%; (j) H_5IO_6, CrO_3, wet MeCN, rt, quant.; (k) HOSu, EDCI·HCl, DCM, rt; (l) cyclic peptide, DIPEA, DMF, rt, **23**: 46% (from **21**), **24**: 25% (from **21**).

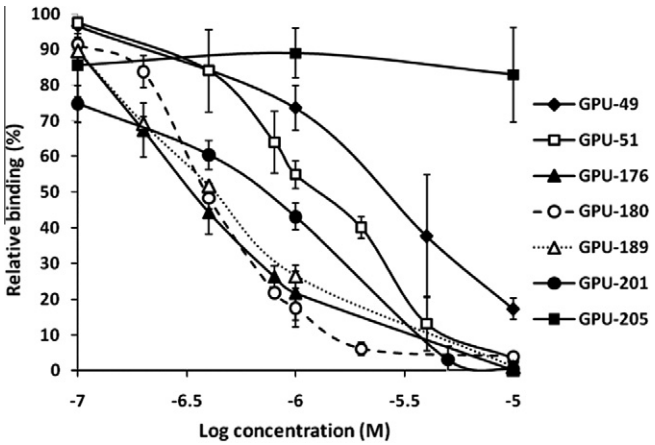

Figure 2. Cell adhesion assay on U87MG cells.

integrin-binding affinity due to the polyvalency effect.[42–44] However, the RGD-monomer GP-176 was found to be the most potent inhibitor among all the conjugates tested here. The difference between GPU-51 and -176 is evident in the structure of the linker. GPU-51 has an ethylene linker derived from β-alanine whereas GPU-176 has cyclohexane linker that is more rigid and longer than the ethylene linker, and restricts the flexibility and orientation of molecule. Although the reason for enhanced binding affinity of GPU-176 is unclear, we suspect it is because its cyclohexane linker kept the boron cluster away from the RGD peptide to enhance recognition of integrin $\alpha_v\beta_3$. BSHs showed slightly higher binding affinity than the corresponding *o*-carborane derivatives. We also performed the cell adhesion assay of GPU-176 and -201 on the mouse cell line SCCVII (squamous cell carcinoma derived from C3H/He mice) expressing integrin $\alpha_v\beta_3$ (Fig. S2 in Supplementary data). The IC_{50} values of GPU-176 and 201 were 0.19 ± 0.08 and 0.68 ± 0.03 μM, respectively. The non-RGD derivative GPU-205 did not inhibit attachment of the cells in the same way as the assay for U87MG.

2.3.2. Biodistribution experiment

We examined RGD-boron cluster conjugates for the time-course of change in boron concentration in solid tumors, brain, blood, liver, muscle, and skin of mice bearing SCCVII tumors. Boron concentrations in tissue were measured by inductively coupled plasma-atomic emission spectroscopy (ICP-AES). All compounds tested here should be enough stable during blood circulation for

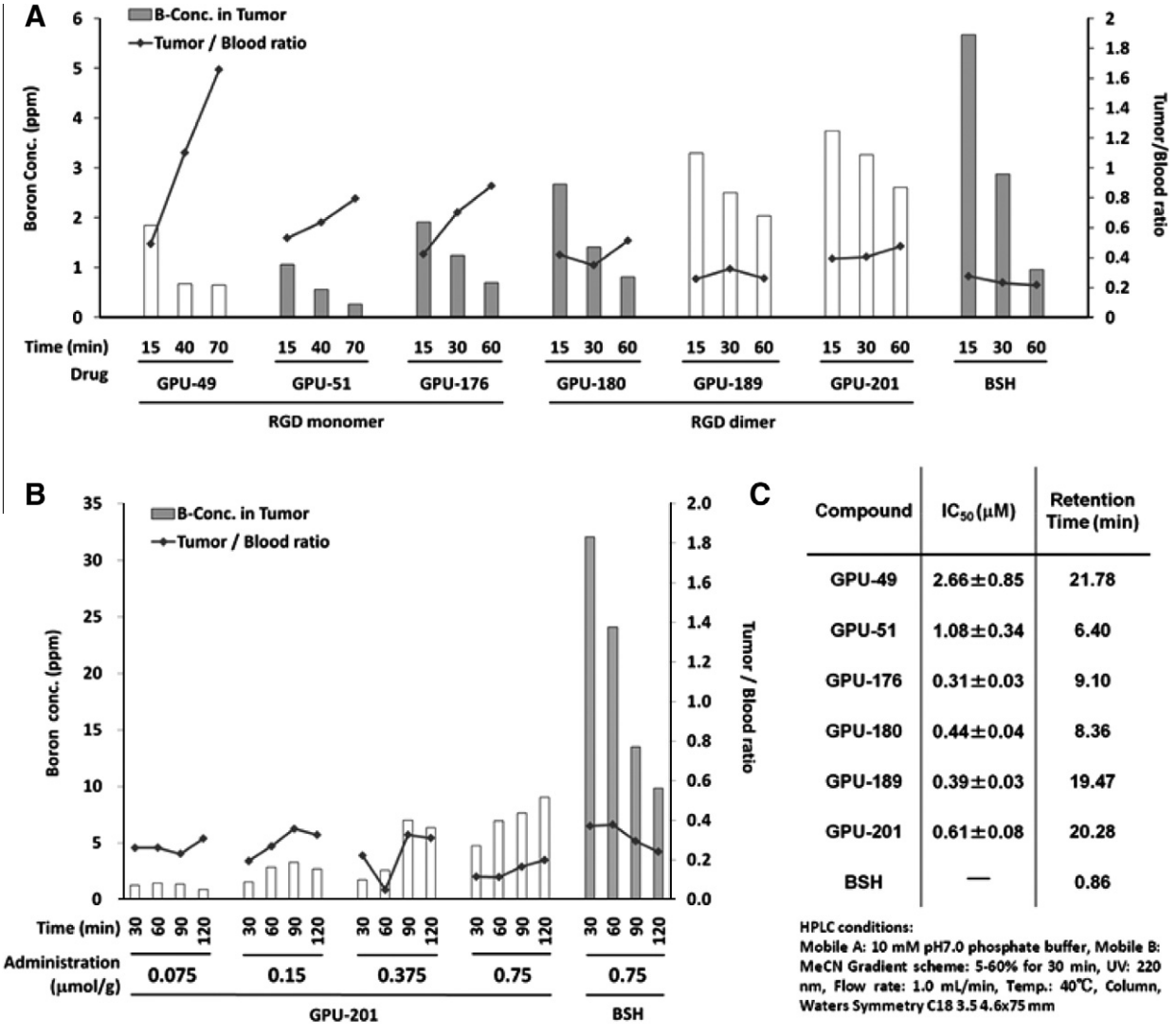

Figure 3. Tumor uptake of RGD conjugates and BSH after intravenous administration at a dose of 0.075 mmol/kg (A) and intraperitoneal administration (B). IC_{50} value in cell adhesion assay on U87MG and retention time on ODS for hydrophobicity analysis (C).

at least 6 h based on the serum stability assay (Fig. S4 in Supplementary data). Figure 3A shows the change in boron concentration in tumors at various time points after intravenous administration of each compound (see also Fig. S3 in Supplementary data for the results in other tissues). All compounds except for BSH were dissolved in physiological (0.9%) saline containing 10% 2-hydroxypropyl-β-cyclodextrin (HP-β-CD) as a solubilizing and dispersing agent, and 0.075 mmol/kg was injected into the tail vein of each mouse. Relatively large intracellular accumulations of boron (approximately 20–30 μg of ^{10}B per gram of tumor) are necessary to produce cell death.[47,48] However the dose of 0.075 mmol/kg in this experiment was one-tenth the dose of BSH (0.75 mmol/kg) previously reported to achieve a boron concentration of >20 μg/g in tumor by intraperitoneally administration.[11] Furthermore, the dosage was also the maximum dose at which a pharmacokinetics response was measured, providing that drug associated toxicity, precipitates and others were not found in case of an intravenous injection. This is because the solubility of RGD-boron clusters in water is relatively low. To evaluate hydrophobicity, all compounds were analyzed by reverse-phase (RP)-HPLC and retention time in gradient mode is shown in Figure 3C. The order of hydrophobicity are predicted by the retention time was GPU-49 > -201 > -189 > -176 > -180 > -51 > BSH, that is, all carborane derivatives were more hydrophobic than BSH derivatives.

Tumor uptake of BSH 15 min following injection was much higher than that in other RGD conjugates, but BSH was rapidly washed out from tumors. In contrast, GPU-201 and -189 (RGD-dimer and *o*-carborane conjugate, respectively) showed good accumulation and retention in tumors. The tumor/blood ratio of GPU-201 was nearly twice greater than that of BSH from 15 min to 60 min following intravenous injection. Dimeric RGD conjugates showed higher boron concentrations in tumors than those of monomeric RGD conjugates. Among dimeric RGD derivatives, GPU-180 including BSH showed the lowest uptake in the same level of monomeric RGD derivatives due to its hydrophilic properties. Although boron concentrations were low in the brain, the concentrations in muscle and skin were similar to those in the tumors whereas those in the blood and liver were much higher than those in the tumors (Fig. S3). In particular, the concentrations of the monomeric RGD derivatives GPU-51 and -49 in the liver were significantly higher irrespective of their hydrophobicity, which might cause to be lower concentration in blood and tumor. Consequently, GPU-201 maintained high boron concentrations in tumors more effectively than any other compound.

We, therefore, examined the dose-dependence of GPU-201 on tumor distribution after intraperitoneal injection (Fig. 3B). The boron concentrations in tumors from 30 min to 120 min following intraperitoneal injection of GPU-201 decreased to one-third of that of BSH intravenous injection because of low bioavailability. However, the tumor retention of boron following intraperitoneal injection was higher than that following intravenous injection. The boron concentrations in tumors at each time point following intraperitoneal injection increased dose-dependently. Interestingly, boron concentrations in tumors increased till 120 min, whereas BSH was eliminated promptly.

Tumor accumulations of dimeric RGD derivatives were higher than those in monomeric RGD derivatives. However, the results did not clarify the direct correlation between in vivo tumor accumulation and in vitro integrin-binding affinity. To maximize BNCT efficiency, the amount of ^{10}B atom accumulated in tumor tissue must be $\geqslant$20 μg/g of tissue with a ratio of tumor/blood concentration of 4:1.[23] Though the tumor retention of boron was significantly improved, the maximum boron concentration was >9 ppm in tumors 120 min after intraperitoneal injection at 0.75 mmol/kg of GPU-201. Due to low water-solubility, administering an adequate dose of the boron conjugate to achieve an efficient boron concentration in tumor for BNCT could not be performed in the present study. Further studies are required to improve the solubility and bioavailability of boron conjugates.

3. Conclusion

We synthesized the cyclic RGD-boron cluster conjugates GPU-49, -51, -176, -180, -189, and -201 to develop tumor-selective boron carriers for BNCT. All RGD conjugates had high in vitro integrin $\alpha_v\beta_3$-binding affinity, and showed dose-dependent inhibition of cell adhesion with IC_{50} values of 0.19–2.66 μM in a vitronectin-mediated cell adhesion assay on U87MG cells and SCCVII cells. By analyses of in vivo biodistribution, RGD dimer-boron clusters had higher tumor uptake and slower clearance than that of monomeric RGD conjugates. In particular, GPU-201 should be a promising candidate due to its dose dependent-tumor uptake and significantly longer tumor retention than BSH. We shall evaluate its radio-sensitizating effect under thermal neutrons beam exposure in future studies.

4. Experimental

4.1. General

Protected amino acids, Cl-Trt(2-Cl) resins were purchased from Novabiochem (Merck). Decaborane (14) ($B_{10}H_{14}$) and ^{10}B-enriched disodium mercaptododecaborate (BSH) were purchased from KatChem. Other reagents were purchased from Sigma–Aldrich, Wako or TCI. RP-HPLC analyses were performed on 10-AD series (Shimadzu) equipped with Waters Symmetry C18 analytical column (Waters, 4.6 × 75 mm, flow rate 1 mL/min). For preparative HPLC, Bensil 5-C18 preparative column (Bentech, 20 × 315 mm, flow rate 6 mL/min) was employed. A solvent system consisting 0.1% TFA solution (v/v) and 0.1% TFA in acetonitrile (v/v) or 10 mM pH 7.0 sodium phosphate buffer and acetonitrile were used for HPLC elution and the eluting products were detected by UV at 220 nm. Microwave reactions were performed on Biotage Initiator 2.0 with single mode operating at 2.45 GHz. Electron impact (EI) or fast atom bombardment (FAB) mass spectra were recorded on a JEOL JMS-SX102A mass spectrometer. High- and low-resolution mass spectra using electron spray ionization (ESI) were obtained on LCMS-IT-TOF (Shimadzu) and HP1100 series (Hewlett-Packard), respectively. ^{1}H and ^{13}C NMR spectra were recorded using a JEOL JNM-AL400 or JNM-EX400 spectrometer at 400 MHz (^{1}H NMR) and 100 MHz (^{13}C NMR) frequency in $CDCl_3$, d_6-DMSO or d_6-Acetone. Chemical shifts for ^{1}H NMR were referenced to tetramethylsilane (0.00 ppm). Chemical shifts for ^{13}C NMR were calibrated to the solvent signals ($CDCl_3$: 77.0 ppm, d_6-DMSO: 39.5 ppm, d_6-Acetone: 29.8 ppm). Infrared (IR) spectra were measured on a JASCO IRA-100. Inductively coupled plasma-atomic emission spectrometry (ICP-AES) analyses were performed on Ultima2 (Horiba-Jobin-Yvon) and the spectra was measured at 249.773 nm.

4.2. Synthesis of c(RGDfK) and c(KGfDR) using solid phase peptide synthesis by Fmoc strategy

Linear-protected peptides were manually constructed on Fmoc-Gly-Trt-resin (0.4–0.6 mmol/g). Fmoc-amino acids were coupled with 3 equiv of *N*,*N*′-diisopropylcarbodiimide and HOBt·H_2O in DMF for 1–2 h. The Fmoc group was deprotected by treatment with 20% (v/v) piperidine in DMF for 20 min. Protected peptide linked to resin was cleaved with 20% (v/v) 1,1,1,3,3,3-hexafluoroisopropanol in DCM for 2 h. Filtration and removal of the solvent gave the crude linear protected peptide. The residue was dissolved in DMF (3 mM solution) and the solution was cooled to −40 °C. Diphenylphospho-

ryl azide (3 equiv) and $NaHCO_3$ (5 equiv) were added to the solution at the same temperature and the solution was stirred for 36 h at room temperature. After filtration and evaporation of the solvent, the residue was charged over basic alumina and eluted with $CHCl_3$/MeOH (9:1) to afford crude protected cyclic peptide. The protected cyclic peptide was deprotected with 95% (v/v) TFA for 2 h at room temperature. After concentration, the residue was purified by preparative RP-HPLC to afford pure cyclic peptide as a bistrifluroacetate salt of colorless freeze-dried amorphous. Yield: c(RGDfK)·2TFA (99%): LRMS (ESI) *m*/*z*: $[M+H]^+$ 604.3, c(KGfDR)·2TFA (42%): HRMS (ESI) *m*/*z*: calcd for $C_{27}H_{41}N_9O_7^+$ $[M+H]^+$ 604.3202, found 604.3210.

4.2.1. *cyclo*[L-Arginyl-L-glycyl-L-asparagyl-D-phenylalanyl-L-(ε*N*-[3-(1-maleimido)propionyl])lysine] trifluoroacetate (2)

To a solution of c(RGDfK)·2TFA (0.333 g, 0.40 mmol) and **1** (0.107 g, 0.40 mmol) in 5 mL of DMF was added *N*,*N*-diisopropylethylamine (DIPEA) (0.279 mL, 1.60 mmol) and the solution was stirred at room temperature. After 24 h, the solvent was removed in vacuo. Purification of the crude product by preparative RP-HPLC afforded **2** (0.293 g, 84%) as trifluoroacetate salt of colorless freeze-dried amorphous. HRMS (FAB) *m*/*z*: calcd for $C_{34}H_{47}N_{10}O_{10}$ $[M+H]^+$ 755.3471, found 755.3485.

4.2.2. *cyclo*[L-Arginyl-L-glycyl-L- asparagyl-D-phenylalanyl-L-(ε *N*-[(1-[3-(undecahydrododecaborato)sulfanyl]succinimido) propionyl])lysine] disodium salt: GPU-51 (3)

The linker conjugated peptide **2** (127 mg, 0.14 mmol) and ^{10}BSH (88.3 mg, 0.42 mmol) were dissolved in 5 mL of 0.2 M sodium phosphate buffer (pH 7.0)/MeCN (= 1:1) solution under N_2 atmosphere and the solution was stirred at room temperature for one day. The reaction solution was charged on a pre-charged resin (Waters OASIS HLB cartridge) and eluted with H_2O/MeCN (100:0–85:15) to give **3** (74.3 mg, 56%) as disodium salt of colorless freeze-dried amorphous. HRMS (ESI) *m*/*z*: calcd for $C_{34}H_{58}{}^{10}B_{12}N_{10}O_{10}S^{2-}$ $[M]^{2-}$ 459.2811, found 459.2811.

4.2.3. Bis[ε*N*′-*cyclo*(L-arginyl-L-glycyl-L-asparagyl-D-phenylalanyl-L-lysyl)] α*N*-[3-(1-maleimido)propionyl]glutamide bistrifluoroacetate (4)

To a solution of E[c(RGDfK)$_2$]·3TFA (143 mg, 0.086 mmol) and **1** (26.6 mg, 0.10 mmol) in 5 mL of DMF was added DIPEA (0.418 mL, 2.40 mmol) and the solution was stirred at room temperature. After 6 h, the solvent was removed in vacuo. Purification of the crude product by preparative RP-HPLC afforded **4** (109 mg, 86%) as bistrifluoroacetate salt of colorless freeze-dried amorphous. HRMS (ESI) *m*/*z*: calcd for $C_{66}H_{93}N_{20}O_{19}^+$ $[M+H]^+$ 1469.6920, found 1469.6906.

4.2.4. Bis[ε*N*′-*cyclo*(L-arginyl-L-glycyl-L-asparagyl-D-phenylalanyl-L-lysyl)] α*N*-[(1-[3-(undecahydrododecaborato) sulfanyl]succinimido)propionyl]glutamide: GPU-180 (5)

The linker conjugated peptide **4** (73.0 mg, 0.043 mmol) and ^{10}BSH (40.0 mg, 0.19 mmol) were dissolved in 4.5 mL of 0.2 M sodium phosphate buffer (pH 7.0)/MeCN (= 8:1) solution under N_2 atmosphere and the solution was stirred at room temperature for two days. Purification of the crude product by preparative RP-HPLC afforded **5** (50 mg, 71%) of colorless freeze-dried amorphous. HRMS (ESI) *m*/*z*: calcd for $C_{66}H_{104}{}^{10}B_{12}N_{20}O_{19}S^-$ $[M]^{2-}$ 816.4535, found 816.4545.

4.2.5. *cyclo*(L-Arginyl-L-glycyl-L-asparagyl-D-phenylalanyl-L-[ε*N*-(*trans*-[4-(1-maleimido)methyl]cyclohexylcarbonyl)]lysine) trifluoroacetate (8)

To a solution of **6** (0.387 g, 1.60 mmol) and *N*-hydroxysuccinimide (HOSu) (0.562 g, 4.90 mmol) in 19.6 mL of DCM was added 1-ethyl-3-(3-dimethylaminopropyl) carbodiimide hydrochloride (EDCI·HCl) (0.939 g, 4.90 mmol) at room temperature and stirred for 4 h. The solvent was removed and the residue was dissolved in ethyl acetate. The solution was washed with 10% citric acid (three times), satd $NaHCO_3$ (three times) and brine, dried over $MgSO_4$ and concentrated to afford crude product **7** which was used without further purification. To a solution of c(RGDfK)·2TFA (50 mg, 0.06 mmol) and **7** (13.4 mg, 0.04 mmol) in 2 mL of DMF was added DIPEA (34.8 μL, 0.20 mmol) and the solution was stirred at room temperature. After 9 h, the solvent was removed in vacuo. Purification of the crude product by preparative RP-HPLC afforded **8** (19.1 mg, 40% for two-steps) as trifluoroacetate salt of colorless freeze-dried amorphous. HRMS (FAB) *m*/*z*: calcd for $C_{39}H_{55}N_{10}O_{10}^+$ $[M+H]^+$ 823.4097, found 823.4091.

4.2.6. *cyclo*(L-Arginyl-L-glycyl-L-asparagyl-D-phenylalanyl-L-[ε*N*-(*trans*-[4-(1-[3-(undecahydrododecaborato)sulfanyl]succimido) methyl]cyclohexylcarbonyl)]lysine) sodium salt: GPU-176 (9)

The linker conjugated peptide **8** (19.0 mg, 0.02 mmol) and ^{10}BSH (12.6 mg, 0.06 mmol) were dissolved in 6 mL of 0.2 M sodium phosphate buffer (pH 7.0)/MeCN (= 2:1) solution under N_2 atmosphere and the solution was stirred at room temperature for 36 h. Purification of the crude product by preparative RP-HPLC afforded **9** (10.6 mg, 45%) as sodium salt of colorless freeze-dried amorphous. HRMS (ESI) *m*/*z*: calcd for $C_{39}H_{66}{}^{10}B_{12}N_{10}O_{10}S^{2-}$ $[M]^{2-}$ 493.3124, found 493.3110.

4.2.7. 1-(4-Benzyloxybutyl)-1,2-dicarba-*closo*-dodecaborane (12)

A 0.5 mL microwave vial equipped with stir bar was charged with 6-benzyloxyhex-1-yne (**11**) (0.20 mmol, 37.6 mg), decaborane (14) (0.20 mmol, 24.4 mg), *N*,*N*-dimethylaniline (48.5 mg, 0.40 mmol) and chlorobenzene (0.4 mL). The solution was stirred for 30 s before microwave irradiation and the reaction vial was capped. The reaction mixture was then heated by microwave irradiation for 30 min at 80 °C. After irradiation, the reaction mixture was cooled and the residual decaborane was decomposed with small amount of methanol. The reaction mixture was purified by silica-gel chromatography (hexane/ethyl acetate/benzene = 100:1:1) to give **12** (53.9 mg, 88%) as a yellow oil. ^{1}H NMR (400 MHz, $CDCl_3$): δ 1.26–3.04 (br m, 10H), 1.50–1.55 (m, 4H), 2.17 (t, *J* = 7.9 Hz, 2H), 3.42 (t, *J* = 5.2 Hz, 2H), 3.48 (br s, 1H), 4.45 (s, 2H), 7.25–7.35 (m, 5H); ^{13}C NMR (100 MHz, $CDCl_3$): δ 26.1, 28.9, 37.7, 60.9, 69.2, 72.9, 75.3, 127.6 (two-Ar carbon was overlapped), 128.4, 138.2.

4.2.8. *N*-Succinimidyl 4-[1-(1,2-dicarba-*closo*-dodecaboranyl)] butanoate (15)

A solution of **14** (130 mg, 0.56 mmol), *N*-hydroxysuccinimide (96.7 mg, 0.84 mmol) and EDCI·HCl (161 mg, 0.84 mmol) in 5 mL of DCM was stirred for 5.5 h at room temperature. The solvent was evaporated, water was added and extracted with ether (three times). The combined organic phase was washed with 10% citric acid (twice), brine, satd $NaHCO_3$ (twice) and brine, dried over $MgSO_4$ and evaporated to afford crude product. Purification by silica-gel column chromatography (hexane/ethyl acetate = 1:1) gave **15** (178 mg, 97%) as a white solid. ^{1}H NMR (400 MHz, $CDCl_3$): δ 1.42–3.14 (m, 10H), 1.91–1.99 (m, 2H), 2.34–2.38 (m, 2H), 2.63 (t, *J* = 6.8 Hz, 2H), 2.84 (s, 4H), 3.65 (br s, 1H); ^{13}C NMR (100 MHz, $CDCl_3$): δ 24.3, 25.6, 30.2, 36.4, 61.7, 74.1, 167.5, 169.0; HRMS (FAB) *m*/*z*: calcd for $C_{10}H_{22}B_{10}NO_4^+$ $[M+H]^+$ 330.2474,, found 330.2468.

4.2.9. *cyclo*(L-Arginyl-L-glycyl-L-asparagyl-D-phenylalanyl-L-[ε*N*-(4-[1-(1,2-dicarba-*closo*-dodecaboranyl)]butanoyl)]lysine) trifluoroacetate: GPU-49 (16)

To a solution of c(RGDfK)·2TFA (49.9 mg, 0.06 mmol) and **15** (29.5 mg, 0.09 mmol) in 0.6 mL of DMF was added DIPEA (42 μL,

0.24 mmol) and the solution was stirred for one day. Purification of the crude product by preparative RP-HPLC afforded **16** (48.1 mg, 86%) as trifluoroacetate salt of colorless freeze-dried amorphous. HRMS (ESI) *m*/*z*: calcd for $C_{33}H_{58}B_{10}N_9O_8^+$ $[M+H]^+$ 818.5333, found 818.5393.

4.2.10. Bis[$^{\varepsilon}$*N*′-*cyclo*(L-arginyl-L-glycyl-L-asparagyl-D-phenylalanyl-L-lysyl)] $^{\alpha}$*N*-(4-[1-(1,2-dicarba-*closo*-dodecaboranyl)] butanoyl)glutamide bistrifluoroacetate: GPU-189 (17)

To a solution of E[c(RGDfK)$_2$]·3TFA (99.6 mg, 0.06 mmol) and **15** (16.4 mg, 0.05 mmol) in 1 mL of DMF was added DIPEA (93 μL, 0.54 mmol) and the solution stirred for 8 h. Purification of the crude product by preparative RP-HPLC afforded **17** (60.2 mg, 68%) as bistrifluoroacetate salt of colorless freeze-dried amorphous. HRMS (ESI) *m*/*z*: calcd for $C_{65}H_{105}B_{10}N_{19}O_{17}^{2+}$ $[M+2H]^{2+}$ 766.4468, found 766.4495.

4.2.11. 1,2-Bis(4-benzyloxybutyl)-1,2-dicarba-*closo*-dodecaborane (19)

To a solution of **12** (61.3 mg, 0.20 mmol) in 2 mL of THF was added dropwise *n*-butyllithium (2.76 M in hexane; 94.2 μL, 0.26 mmol) under Ar atmosphere at −40 °C and the reaction was warmed to room temperature. Lithium iodide (5.3 mg, 0.04 mmol) in 0.4 mL of THF and **18** (63.2 mg, 0.26 mmol) in 1 mL of THF were successively added and the mixture was stirred overnight at room temperature. The reaction was quenched with water and the product was extracted with ether. The organic phase was washed with water, brine and then dried over $MgSO_4$ and concentrated under reduced pressure. The residue was purified by preparative-TLC with hexane/ethyl acetate (10:1) to afford **19** (60.8 mg, 65%) as a yellow oil. ^{1}H NMR (400 MHz, $CDCl_3$): δ 7.35–7.31 (m, 10 H), 4.74 (s, 4 H), 3.43 (t, J = 6.0 Hz, 4 H), 2.13–2.12 (m, 4 H), 1.59–1.57 (m, 8 H), 2.79–1.34 (br m, 10 H); ^{13}C NMR (100 MHz, $CDCl_3$): δ 165.8, 138.2, 128.4, 127.6, 79.7, 73.0, 64.5, 34.8, 29.2, 26.7; HRMS (EI) *m*/*z*: calcd for $C_{24}H_{40}{}^{10}B_{10}$ $[M]^+$ 468.4026, found 468.4034.

4.2.12. 1,2-Bis(4-hydroxybutyl)-1,2-dicarba-*closo*-dodecaborane (20)

A mixture of **19** (93.7 mg, 0.20 mmol), 10% Pd/C (42.6 mg, 0.04 mmol), cyclohexene (2 ml), and ethanol (4 mL) was refluxed overnight. The mixture was then filtered with celite pad and concentrated under reduced pressure to give **20** (50.9 mg, 88%) as a white solid. ^{1}H NMR (400 MHz, d_6-Acetone): δ 3.58–3.55 (t, J = 6.1 Hz, 4H), 2.40–2.36 (m, 4H), 1.70–1.62 (m, 4H), 1.58–1.51 (m, 4H), 4.48–1.00 (m, 10H); ^{13}C NMR (100 MHz, d_6-Acetone): 81.8, 61.6, 35.3, 32.7, 27.2; HRMS (EI) *m*/*z*: calcd for $C_{10}H_{28}B_{10}O_2^+$ $[M^+]$ 290.3014, found 290.3020.

4.2.13. 1,2-Dicarba-*closo*-dodecaboranedibutanoic acid (21)

To a solution of **20** (419 mg, 1.45 mmol) in 16.5 mL of wet MeCN was added dropwise 16.5 mL of the H_5IO_6/CrO_3 solution in an ice bath.[46] The solution was stirred for 2 h at 0 °C and overnight at room temperature. The reaction mixture was purified by RP-HPLC to give **21** (458 mg, quant.) as colorless freeze-dried amorphous. ^{1}H NMR (400 MHz, d_6-Acetone): δ 1.21–3.05 (m, 10H), 1.68–1.75 (m, 4H), 2.24–2.33 (m, 8H), 10.43 (br s, 1H); ^{13}C NMR (100 MHz, d_6-Acetone): 25.6, 32.8, 34.5, 81.3, 174.0; HRMS (ESI) *m*/*z*: calcd for $C_{10}H_{25}{}^{10}B_{10}O_4^+$ $[M+H]^+$ 309.3041, found 309.3049.

4.2.14. Bis[$^{\varepsilon}$*N*′-*cyclo*(L-arginyl-L-glycyl-L-asparagyl-D-phenylalanyl-L-lysyl)] 1,2-dicarba-*closo*-dodecaboranedibutanamide bistrifluoroacetate: GPU-201 (23)

To a solution of **21** (458 mg, 1.45 mmol) and HOSu (460 mg, 4.0 mmol) in 40 mL of DCM was added EDCI·HCl (767 mg, 4.0 mmol) at room temperature and stirred for 12 h. The solvent was removed and the residue was dissolved in ethyl acetate. The solution was washed with 10% citric acid (three times), satd $NaHCO_3$ (three times) and brine, dried over $MgSO_4$ and concentrated to afford crude di-activated ester **22**. To a solution of **22** (crude 80 mg) and c(RGDfK)·2TFA (416 mg, 0.50 mmol) in 3 mL of DMF was added DIPEA (0.372 mL, 2.14 mmol) and stirred for 12 h at room temperature. The solvent was removed in vacuo and the residue was purified by preparative RP-HPLC to afford **23** (121 mg, 46% from **21**) as bistrifluoroacetate salt of colorless freeze-dried amorphous. HRMS (ESI) *m*/*z*: calcd for $C_{64}H_{104}B_{10}N_{18}O_{16}^{2+}$ $[M+2H]^{2+}$ 745.4399, found 745. 4447.

4.2.15. Bis[$^{\varepsilon}$*N*′-*cyclo*(L-lysyl-L-glycyl-D-phenylalanyl-L-asparagyl-L-arginyl)] 1,2-dicarba-*closo*-dodecaboranedibutanamide bistrifluoroacetate: GPU-205 (24)

To a solution of **22** (51.1 mg, 0.10 mmol) and c(KGfDR)·2TFA (249 mg, 0.30 mmol) in 7 mL of DMF was added DIPEA (174 μL, 1.0 mmol) and the reaction mixture was stirred overnight at room temperature. The solvent was removed in vacuo and the residue was purified by preparative RP-HPLC to afford **24** (43.1 mg, 25% from **21**) as bistrifluoroacetate salt of colorless freeze-dried amorphous. HRMS (ESI) *m*/*z*: calcd for $C_{64}H_{104}B_{10}N_{18}O_{16}^{2+}$ $[[M+2H]^{2+}$ 745.4399, found 745.4458.

4.3. Cell adhesion assay

Ninety-six-well culture plates were coated with 100 μL of 2 μg/mL vitronectin (AGC Techno Glass) in PBS at 4 °C overnight, and treated with 2% bovine serum albumin (BSA) (Wako) in PBS. U87MG cells or SCCVII cells were suspended at 2×10^5 cells/mL in Minimum Essential Medium Eagle (MEM) (Sigma–Aldrich) containing 1 mM $MgCl_2$, 0.25 mM $MnSO_4$, and 0.1% BSA. The suspension was incubated with varying concentrations of RGD conjugates for 20 min at 37 °C. Hundred microliter per well (2×10^4 cells) were added to the wells and incubated for 1 h at 37 °C. The wells were washed three times with PBS. Adherent cells were then fixed for 15 min with 10% formalin and stained with 0.04% crystal violet. Plates were washed three times with distilled water and the remaining bound dye was solubilized in 100 μL of 1% SDS (Wako) for 1 h. The number of cells was then evaluated by measuring absorbance at 570 nm with a microplate reader.

4.3.1. Mice and tumors

SCCVII squamous cell carcinoma derived from C3H/He mice was maintained in vitro in MEM (Sigma–Aldrich) containing 12.5% FBS (Japan Bioserum). Cells were collected from exponentially growing cultures, and 1×10^5 cells of each tumor were inoculated subcutaneously into both hind legs of 8–11-week-old syngeneic female C3H/He mice (Japan Animal). Fourteen days after inoculation, each tumor was approximately 1 cm in diameter. Mice were handled according to the Recommendations for Handling of Laboratory Animals for Biomedical Research, complied by the Committee on Safety and Ethical Handling Regulations for Laboratory Animal Experiments, Kyoto University. All experimental procedures mentioned here were in accordance with institutional guidelines for the care and use of laboratory animals in research.

4.3.2. Biodistribution experiments

All compounds were dissolved in physiological saline containing 10% HP-β-cyclodextrin (Nisshoku). They were administered to the tumor-bearing mice via the intravenous or intraperitoneal route. BSH dissolved in physiological saline was administrated intravenously or intraperitoneally. At various time points following BSH administration, mice were killed, and tumors and certain organs were collected and weighed. Samples (0.2–0.5 g) in polyethylene vials were treated with 70% perchloric acid and 30% hydrogen peroxide. The vials were then placed in shaking water bath for 24 h

at 75 °C. The volume of the samples was precisely adjusted to 5–10 μL with distilled water. The solutions were then filtered through a 0.22-μm filter. Boron concentrations in the solution were measured by ICP-AES.

Acknowledgments

This research was supported in part by a Grant from The Saijiro Endo Memorial Foundation for Science & Technology, the Sasagawa Scientific Research Grant from The Japan Science Society (19-621), and a Grant-in-Aid for Scientific Research (C) (19590102) from the Japan Society for the Promotion of Science. The authors thank Prof. Osamu Sakurada at Gifu University for the use of ICP-AES, Prof. Mitsunori Kirihata at Osaka Prefecture University for helpful suggestions about ICP-AES, and Ms. Emi Inaba for their technical assistance.

Supplementary data

Supplementary data associated with this article can be found, in the online version, at doi:10.1016/j.bmc.2011.01.020.

References and notes

1. Soloway, A. H.; Tjarks, W.; Barnum, B. A.; Rong, F. G.; Barth, R. F.; Codogni, I. M.; Wilson, J. G. *Chem. Rev.* **1998**, *98*, 1515.
2. Hawthorne, M. F. *Angew. Chem., Int. Ed.* **1993**, *32*, 950.
3. Soloway, A. H.; Hatanaka, H.; Davis, M. A. *J. Med. Chem.* **1967**, *10*, 714.
4. Nakagawa, Y.; Hatanaka, H. *J. Neurooncol.* **1997**, *33*, 105.
5. Snyder, H. R.; Reedy, A. J.; Lennarz, W. J. *J. Am. Chem. Soc.* **1958**, *80*, 835.
6. Mishima, Y.; Ichihashi, M.; Hatta, S.; Honda, C.; Yamamura, K.; Nakagawa, T. *Pigment Cell Res.* **1989**, *2*, 226.
7. Wittig, A.; Collette, L.; Appelman, K.; Buhrmann, S.; Jackel, M. C.; Jockel, K. H.; Schmid, K. W.; Ortmann, U.; Moss, R.; Sauerwein, W. A. *J. Cell. Mol. Med.* **2009**, *13*, 1653.
8. Gottumukkala, V.; Luguya, R.; Fronczek, F. R.; Vicente, M. G. H. *Bioorg. Med. Chem.* **2005**, *13*, 1633.
9. Wittig, A.; Huiskamp, R.; Moss, R. L.; Bet, P.; Kriegeskotte, C.; Scherag, A.; Hilken, G.; Sauerwein, W. A. G. *Radiat. Res.* **2009**, *172*, 493.
10. Masunaga, S.; Nagasawa, H.; Hiraoka, M.; Sakurai, Y.; Uto, Y.; Hori, H.; Nagata, K.; Suzuki, M.; Maruhashi, A.; Kinashi, Y.; Ono, K. *Anticancer Res.* **2004**, *24*, 2975.
11. Masunaga, S.; Nagasawa, H.; Gotoh, K.; Sakurai, Y.; Uto, Y.; Hori, H.; Nagata, K.; Suzuki, M.; Maruhashi, A.; Kinashi, Y.; Ono, K. *Radiat. Med.* **2006**, *24*, 98.
12. Nagasawa, H. *J. Pharm. Sci.* **2011**, in press.
13. Mier, W.; Gabel, D.; Haberkorn, U.; Eisenhut, M. *Z. Anorg. Allg. Chem.* **2004**, *630*, 1258.
14. Betzel, T.; Hess, T.; Waser, B.; Reubi, J. C.; Roesch, F. *Bioconjugate Chem.* **2008**, *19*, 1796.
15. Shukla, S.; Wu, G.; Chatterjee, M.; Yang, W. L.; Sekido, M.; Diop, L. A.; Muller, R.; Sudimack, J. J.; Lee, R. J.; Barth, R. F.; Tjarks, W. *Bioconjugate Chem.* **2003**, *14*, 158.
16. Wu, G.; Barth, R. F.; Yang, W.; Lee, R. J.; Tjarks, W.; Backer, M. V.; Backer, J. M. *Anticancer Agents Med. Chem.* **2006**, *6*, 167.
17. Miyajima, Y.; Nakamura, H.; Kuwata, Y.; Lee, J. D.; Masunaga, S.; Ono, K.; Maruyama, K. *Bioconjugate Chem.* **2006**, *17*, 1314.
18. Thirumamagal, B. T. S.; Zhao, X. B.; Bandyopadhyaya, A. K.; Narayanasamy, S.; Johnsamuel, J.; Tiwari, R.; Golightly, D. W.; Patel, V.; Jehning, B. T.; Backer, M. V.; Barth, R. F.; Lee, R. J.; Backer, J. M.; Tjarks, W. *Bioconjugate Chem.* **2006**, *17*, 1141.
19. Pan, X. G.; Wu, G.; Yang, W. L.; Barth, R. F.; Tjarks, W.; Lee, R. J. *Bioconjugate Chem.* **2007**, *18*, 101.
20. Yang, W. L.; Barth, R. F.; Wu, G.; Huo, T. Y.; Tjarks, W.; Ciesielski, M.; Fenstermaker, R. A.; Ross, B. D.; Wikstrand, C. J.; Riley, K. J.; Binns, P. J. *J. Neurooncol.* **2009**, *95*, 355.
21. Byun, Y.; Narayanasamy, S.; Johnsamuel, J.; Bandyopadhyaya, A. K.; Tiwari, R.; Al-Madhoun, A. S.; Barth, R. F.; Eriksson, S.; Tjarks, W. *Anticancer Agents Med. Chem.* **2006**, *6*, 127.
22. Kabalka, G. W.; Yao, M. L. *Anticancer Agents Med. Chem.* **2006**, *6*, 111.
23. Renner, M. W.; Miura, M.; Easson, M. W.; Vicente, M. G. *Anticancer Agents Med. Chem.* **2006**, *6*, 145.
24. Ratajski, M.; Osterloh, J.; Gabel, D. *Anticancer Agents Med. Chem.* **2006**, *6*, 159.
25. Bregadze, V. I.; Sivaev, I. B.; Glazun, S. A. *Anticancer Agents Med. Chem.* **2006**, *6*, 75.
26. Desgrosellier, J. S.; Cheresh, D. A. *Nat. Rev. Cancer* **2010**, *10*, 9.
27. Hynes, R. O. *Cell* **1992**, *69*, 11.
28. Hood, J. D.; Cheresh, D. A. *Nat. Rev. Cancer* **2002**, *2*, 91.
29. Brooks, P. C.; Clark, R. A.; Cheresh, D. A. *Science* **1994**, *264*, 569.
30. Cao, Q.; Li, Z.; Chen, K.; Wu, Z.; He, L.; Neamati, N.; Chen, X. *Eur. J. Nucl. Med. Mol. Imag.* **2008**, *35*, 1489.
31. Beer, A. J.; Schwaiger, M. *Cancer Metastasis Rev.* **2008**, *27*, 631.
32. Wangler, C.; Maschauer, S.; Prante, O.; Schafer, M.; Schirrmacher, R.; Bartenstein, P.; Eisenhut, M.; Wangler, B. *ChemBioChem* **2010**, *11*, 2168.
33. Li, Z.; Cai, W.; Cao, Q.; Chen, K.; Wu, Z.; He, L.; Chen, X. *J. Nucl. Med.* **2007**, *48*, 1162.
34. Wu, Z.; Li, Z.; Chen, K.; Cai, W.; He, L.; Chin, F.; Li, F.; Chen, X. *J. Nucl. Med.* **2007**, *48*, 1536.
35. Shi, J.; Kim, Y.; Chakraborty, S.; Jia, B.; Wang, F.; Liu, S. *Bioconjugate Chem.* **2009**, *20*, 1559.
36. Yang, J. Q.; Guo, H. X.; Padilla, R. S.; Berwick, M.; Miao, Y. B. *Bioorg. Med. Chem.* **2010**, *18*, 6695.
37. Chakraborty, S.; Shi, J.; Kim, Y.; Zhou, Y.; Jia, B.; Wang, F.; Liu, S. *Bioconjugate Chem.* **2010**, *21*, 969.
38. Ye, Y.; Bloch, S.; Xu, B.; Achilefu, S. *Bioconjugate Chem.* **2008**, *19*, 225.
39. Wu, Y.; Cai, W.; Chen, X. *Mol. Imag. Biol.* **2006**, *8*, 226.
40. Lee, H.; Li, Z.; Chen, K.; Hsu, A.; Xu, C.; Xie, J.; Sun, S.; Chen, X. *J. Nucl. Med.* **2008**, *49*, 1371.
41. Aumailley, M.; Gurrath, M.; Müller, G.; Calvete, J.; Timpl, R.; Kessler, H. *FEBS Lett.* **1991**, *291*, 50.
42. Liu, S. *Bioconjugate Chem.* **2009**, *20*, 2199.
43. Thumshirn, G.; Hersel, U.; Goodman, S. L.; Kessler, H. *Chem. Eur. J.* **2003**, *9*, 2717.
44. Dijkgraaf, I.; Kruijtzer, J.; Liu, S.; Soede, A.; Oyen, W.; Corstens, F.; Liskamp, R.; Boerman, O. *Eur. J. Nucl. Med. Mol. Imag.* **2007**, *34*, 267.
45. Misra, A. *Bioorg. Med. Chem. Lett.* **2007**, *17*, 3749.
46. Zhao, M.; Li, J.; Song, Z.; Desmond, R.; Tschaen, D. M.; Grabowski, E. J. J.; Reider, P. J. *Tetrahedron Lett.* **1998**, *39*, 5323.
47. Barfh, R. F.; Soloway, A. H.; Fairchild, R. G.; Brugger, R. M. *Cancer* **1992**, *70*, 2995.
48. Justus, E.; Awad, D.; Hohnholt, M.; Schaffran, T.; Edwards, K.; Karlsson, G.; Damian, L.; Gabel, D. *Bioconjugate Chem.* **2007**, *18*, 1287.